Excitation transfer processes in a phosphor-doped poly(*p*-phenylene vinylene) light-emitting diode

I. H. Campbell and D. L. Smith
Materials Science and Technology Division, Los Alamos National Laboratory, Los Alamos, New Mexico 87545

S. Tretiak and R. L. Martin
Theoretical Division, Los Alamos National Laboratory, Los Alamos, New Mexico 87545

C. J. Neef and J. P. Ferraris
Department of Chemistry, The University of Texas at Dallas, Richardson, Texas 75083

(Received 4 September 2001; published 8 February 2002)

We present experimental measurements and theoretical calculations of the electrical and optical properties of phosphor-doped poly (*p*-phenylene vinylene) light-emitting diodes to determine the excitation processes that lead to radiative recombination from the phosphor molecule. Three possible phosphor excitation processes are considered: (1) sequential electron and hole capture by the phosphor, (2) energy transfer from the polymer triplet exciton (Dexter transfer), and (3) energy transfer from the polymer singlet exciton (Förster transfer). The properties of the doped polymer are investigated for doping levels up to about 20 wt %. At the highest doping density, all radiative recombination occurs in the phosphor molecule and the observed electroluminescence decay time increases significantly compared to the undoped polymer. Built-in potential and current-voltage measurements indicate that the electron and hole energy levels of the phosphor are outside the energy gap of the polymer, and that the phosphor molecule does not capture either individual electrons or holes. Measurements of triplet optical absorption show that the triplet population in the polymer is not affected by the presence of the phosphor, indicating that Dexter transfer processes are weak. Calculations of the triplet optical-absorption cross section combined with the measurements of the triplet optical absorption determine the triplet exciton density in the device. In an analogous chemically substituted polymer, no significant excitation transfer occurs when there is no overlap between the emission spectrum of the polymer and the absorption spectrum of the phosphor. These results demonstrate that the dominant excitation transfer path from the polymer to the phosphor is dipole-dipole (Förster) coupling. Calculations of the charged and neutral electronic excitation energies of the polymer and phosphor are performed using hybrid and time-dependent, density-functional theory. The results of these calculations show why Förster transfer is strong in this system, and why the other two transfer processes do not take place.

DOI: 10.1103/PhysRevB.65.085210 PACS number(s): 73.61.Ph, 71.20.Rv, 72.80.Le

I. INTRODUCTION

The most efficient organic light-emitting diodes (LED's) use organic layers doped with phosphorescent molecules.[1–4] The phosphor dopant increases the device quantum efficiency because it has a high quantum yield, and it allows radiative recombination of triplet excitations that would otherwise recombine nonradiatively.[1–4] In these doped organic diodes, electrons and holes are initially injected into the organic host material, and then the excitation is transferred to the dopant producing the phosphorescent excited state. There are three basic methods to produce the phosphorescent excited state in the dopant: sequential charge transfer from the host, energy transfer from host triplet excitons, and energy transfer from host singlet excitons. In the charge-transfer process the electron and hole are captured sequentially by the dopant, leading to the creation of a phosphorescent excitation. In energy-transfer processes, the electron and hole first combine in the host, producing either a triplet or singlet exciton, and then the energy of this excitation is transferred to the dopant by Dexter or Förster processes, respectively. Energy conservation limits the allowed excitation transfer processes. Therefore, the relevant processes can be determined from the charged and neutral electronic excitation energies of the dopant and host, which can be calculated using quantum-chemical techniques. It is important to understand the excitation transfer processes in these doped organic systems in order to design appropriate phosphor molecules and organic hosts to optimize organic LED's.

This paper presents experimental measurements and theoretical calculations of the electrical and optical properties of phosphor doped poly (*p*-phenylene vinylene) light-emitting diodes to determine the excitation processes that lead to radiative recombination from the phosphor molecule. The soluble, conjugated polymer poly [2,5-bis(cholestanoxy)-1,4-phenylene vinylene] (BCHA) was used as the host material and the small molecule 2, 3, 7, 8, 12, 13, 17, 18-octaethyl-21*H*,23*H*-porphine platinum (PtOEP) was used as the dopant. The properties of the doped BCHA were investigated for PtOEP doping levels up to about 20 wt %. At the highest doping density, essentially all radiative recombination occurs in the phosphor molecule and the observed radiative decay time significantly increases. Built-in potential and current-voltage measurements indicate that the electron and hole energy levels of PtOEP are outside the energy gap of BCHA, and that the phosphor is not charged by unipolar current

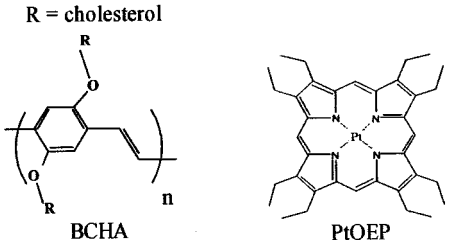

FIG. 1. Chemical structure of BCHA-PPV (left) and PtOEP (right).

flow. This demonstrates that sequential charge capture by the dopant does not occur. Measurements of triplet optical absorption show that the triplet population in BCHA is not affected by the presence of the phosphor, indicating that Dexter transfer processes are weak. No excitation transfer occurs when a related, chemically substituted polymer with a slightly redshifted emission spectrum that does not overlap the dopant absorption spectrum is used. Together, these results demonstrate that the dominant active excitation transfer path from BCHA to PtOEP is Förster transfer. These conclusions are consistent with the charged and neutral electronic excitation energies of BCHA and PtOEP model systems determined by hybrid and time-dependent, density-functional-theory calculations.

The structure of this paper is as follows. Section II presents the basic material and device properties. Section III presents the results of quantum-chemical molecular calculations. Section IV discusses measurements of the excitation transfer mechanisms. Section V summarizes the conclusions.

II. MATERIAL AND DEVICE PROPERTIES

The chemical structures of BCHA and PtOEP are shown in Fig. 1. BCHA is a member of the extensively studied poly (*p*-phenylene vinylene) family of polymers[5–7] and PtOEP has been widely used in phosphorescent LED's.[8,9] The devices consisted of a 150-nm-thick doped or undoped BCHA film sandwiched between a thin, semitransparent Pt or Al electrodes and a thick Ca contact. The fabrication procedures and device geometry were described previously.[10] The Pt/Ca structures are hole dominant, bipolar devices, and the Al/Ca structures are electron only, unipolar devices.[11] These device structures are weak microcavities. Strong microcavities can significantly influence dipole-dipole coupling processes occurring in the film.[12,13]

Figure 2 shows the absorbance (solid) and photoluminescence or electroluminescence (dashed) spectra of: a BCHA film on glass (upper panel), a PtOEP solution (center panel), and a BCHA:PtOEP (20 wt % PtOEP) Pt/Ca diode (lower panel). The absorption and photoluminescence spectra of the BCHA film (upper panel) have broad peaks about 0.5 eV wide that overlap by about 0.2 eV. Cavity effects in these structures are weak and the optical spectra of polymer blend films in the Pt/Ca diode are equivalent to similar spectra of bare films on glass. The absorption and emission spectra of PtOEP are about 0.1 eV wide, and separated by about 0.3 eV. The emission spectrum of BCHA overlaps the absorption

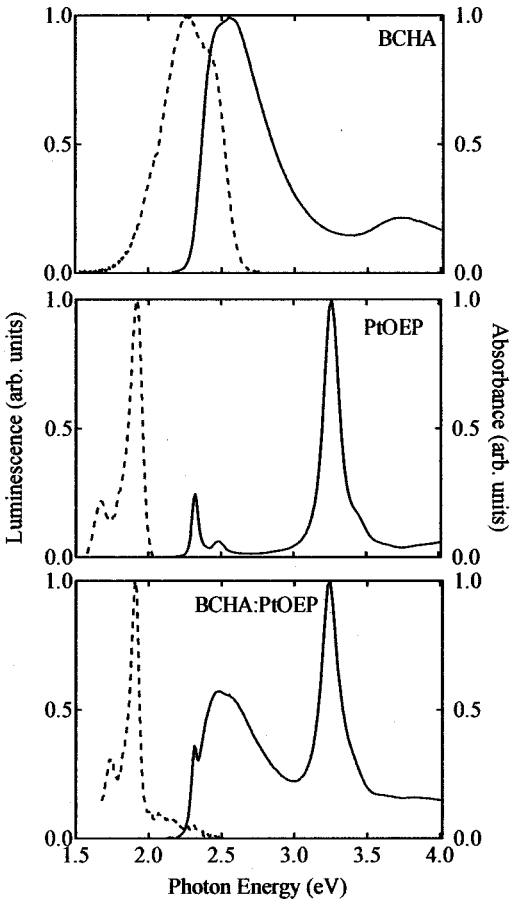

FIG. 2. Measured photoluminescence or electroluminescence (dashed, left vertical axis) and absorbance (solid, right vertical axis) for a BCHA film on a glass substrate (upper panel), a PtOEP solution (center panel) and a BCHA:PtOEP (20 wt %) Pt/Ca diode (lower panel).

spectrum of PtOEP, and therefore Förster energy transfer processes are allowed. The absorption spectrum of the BCHA:PtOEP device is essentially the weighted sum of the absorption spectra of the BCHA and PtOEP molecules. The electroluminescence from the diode structure is dominated by the emission from the PtOEP molecule. The electroluminescence and photoluminescence spectra of BCHA:PtOEP devices are essentially identical (not shown). The luminescence spectrum of these films depends strongly on the PtOEP concentration; at 20 wt % the spectrum is dominated by PtOEP emission, but at 7 wt % the spectrum is roughly one-half BCHA emission and one-half PtOEP emission.

Figure 3 shows the electroluminescence as a function of time for doped (solid) and undoped (dashed) Pt/Ca diodes excited by a 1-μs electrical pulse. The rise and fall times of the electrical pulse were about 15 ns. The luminescence from the undoped diode decreases by one order of magnitude less than 1 μs after the end of the pulse (limited by the luminescence detection scheme). This is consistent with the roughly 1-ns intrinsic radiative lifetime of BCHA singlet excitons. The electroluminescence from the doped sample increases and decreases much more slowly, consistent with long lifetime [$>100\mu$s (Ref. 14)], phosphorescent emission from

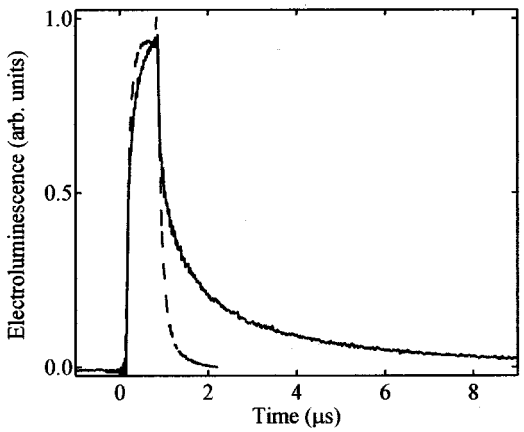

FIG. 3. Time-resolved electroluminescence from a BCHA Pt/Ca diode (dashed line) and a BCHA:PtOEP (20 wt %) Pt/Ca diode (solid line).

PtOEP. Therefore, both spectral and time-resolved electroluminescence measurements demonstrate that PtOEP is the dominant luminescent center in the diode.

III. MOLECULAR CALCULATIONS

Molecular calculations of the electronic properties of BCHA and PtOEP model systems were performed to serve as a basis for understanding the excitation transfer mechanisms occurring in the diode structure. The BCHA model system is identical to BCHA except that the side group is $R=CH_3$ (see Fig. 1) instead of the large R=cholesterol groups. These nonconjugated side groups primarily affect the polymer solubility and not its electronic structure. Several oligomers in this series were studied, and for each the ground-state geometry was optimized using the hybrid B3LYP density functional[15] and the 6-31G basis set. At the optimum geometry, theoretical excitation energies were determined with time-dependent density functional theory (TDDFT).[16–20] For these excited-state calculations, the basis set was improved to 6-31G*, a modification which augments the 6-31G basis with a set of *d* functions on each carbon and oxygen to allow for the possibility of orbital polarization.

Pt(porphyrin) was used as a model system for PtOEP. The Pt(porphyrin) calculations again utilized the B3LYP approximation, and the 6-31G and 6-31G* bases on the porphyrin ligand for optimization and excited-state calculations, respectively. The LANL2 relativistic effective core potential and associated double-zeta basis set were used for the Pt center. The basis set was, however, completely uncontracted, and augmented with an *f*-type polarization function ($\alpha=0.6$). These modifications lead to a $(5s5p3d1f)$ Pt basis set. All calculations utilized the GAUSSIAN98 suite.[21]

The molecular ionization potential (IP) and electron affinity (EA) for the $n=5$ oligomer and Pt(porphyrin) are reported in Table I. These IP and EA values are for isolated molecules. They differ from the IP and EA values of the corresponding solid films because of the large solid state polarization corrections.[22] However, they can be used to compare the relative energies of the solid-state charged excitations of the host and the dopant because the polarization corrections for the oligomer (surrounded by other oligomers) and the Pt(porphyrin) (also surrounded by oligomers) should be similar.[22]

The vertical excitation energies computed for the various oligomers are reported in Table I, and plotted as a function of oligomer length n in Fig. 4. Note that the $S_0 \rightarrow S_1$ excitation energy, where S_0 is the singlet ground state and S_1 is the first singlet excited state, decreases dramatically for the first few members of the series. It is approximately 3.5 eV for the dimer, decreasing to about 2.2 eV for the seven-unit oligomer, and extrapolates to about 2.1 eV for an infinite chain. Similar behavior is observed for the triplet state. In the dimer, it is stabilized by about 1.3 eV relative to the singlet. This difference is somewhat smaller ($\sim$0.8 eV) in the seven-unit oligomer. The large difference between singlet and triplet energies is sometimes associated with large ''electron correlation'' effects, but here it is likely simply a manifestation of the exchange integral between the highest occupied and lowest unoccupied molecular orbitals (HOMO and LUMO) of the oligomer. In the Hartree-Fock approximation, if it is assumed the orbitals do not relax in the excited states, the excitation energies to the first singlet and triplet states are given by

$$\Delta E = \varepsilon_{\mathrm{LUMO}} - \varepsilon_{\mathrm{HOMO}} \pm K_{\mathrm{HOMO,LUMO}}, \qquad (1)$$

where ε is the ground state orbital energy, K is the exchange integral, and the plus (minus) sign is for the singlet (triplet). Because the exchange integral K can be shown to be positive, the triplet is expected to lie lower than the singlet by 2 K. The exchange integral should decrease as the HOMO's and LUMO's delocalize with increasing oligomer length, and this is likely the origin of the trend seen here. This relation-

TABLE I. Selected energetic properties (eV) computed with TDDFT/B3LYP and the basis sets discussed in the text. For the dipole-allowed transitions, the oscillator strengths are given in parentheses.

	(BCHA model)$_n$				
Property	$n=2$	$n=3$	$n=5$	$n=6$	PtP
$S_o \rightarrow S_1$	3.54(0.62)	2.95(1.58)	2.42(3.18)	2.37(3.50)	2.49(0.014)
$S_o \rightarrow T_1$	2.19	1.79	1.54	1.53	1.98
$T_1 \rightarrow T_N$	2.58(1.18)	1.88(1.76)	1.27(3.08)	1.23(3.14)	
IP			5.45		7.01
EA			1.10		1.12

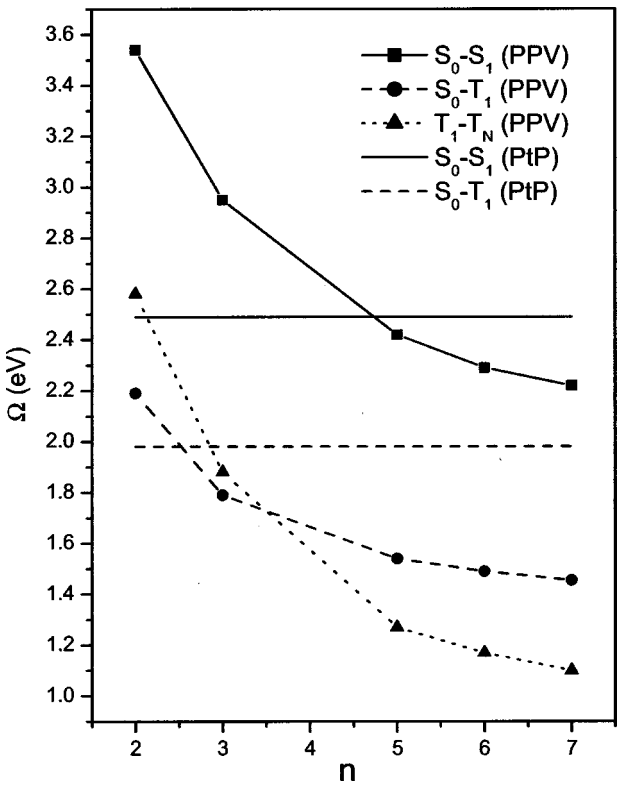

FIG. 4. Calculated vertical excitation energies of Pt(porphyrin) (horizontal lines) and the BCHA model oligomers as a function of oligomer length *n*.

ship is not strictly valid for TDDFT, but it is a useful interpretive model and is consistent with our more detailed calculations.

We also present in Fig. 4 the excitation energy computed for the $T_1 \rightarrow T_N$ transition: $1^3B_u \rightarrow N^3A_g$. The oscillator strength from the lowest triplet excited state, T_1 to higher-lying triplet excited states is strongly concentrated in one specific state which we refer to as T_N. The higher-lying triplet state is the triplet analog of the low-lying A_g singlet studied extensively in the polyene literature.[23,24] The T_N state lies about 2.6 eV above the lowest triplet in the dimer, the difference rapidly decreasing to about 1.1 eV in the seven-unit oligomer. In this evolution, the index "*N*" varies from $N=9$ in the dimer to $N=6$ in the seven-unit oligomer. During this progression, the orbital character of the T_N state remains the same, but the energy of the state moves relative to other triplet states with small oscillator strength to T_1. Oscillator strengths computed for the transition are presented in Table I. The oscillator strengths for $T_1 \rightarrow T_N$ transitions are approximate, and obtained using the $S_0 \rightarrow T_1$ and $S_0 \rightarrow T_N$ transition densities which account for the dominant particle-hole contributions to the oscillator strength. The weaker contribution from higher order electronic correlations included in TDDFT are not taken into account.[25]

The experimental values for the various transitions are roughly $T_1 - S_0 = 1.3$ eV,[26] $S_1 - S_0 = 2.5$ eV,[27] and $T_N - T_1 = 1.5$ eV.[26,27] Our theoretical results extrapolated to infinite chain length are generally somewhat smaller than these numbers. However, the calculated values are in reasonably good

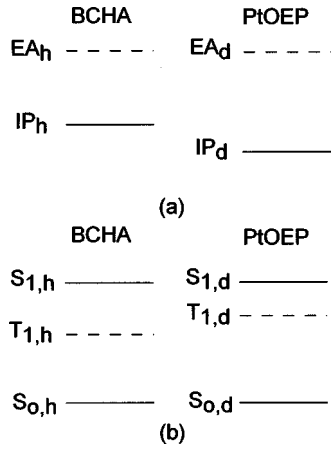

FIG. 5. Schematic electron energy (a) and neutral excitation (b) diagrams for BCHA and PtOEP.

agreement with experiment for an oligomer length $n=5$. One might conclude that either the TDDFT results systematically underestimate these excitation energies or that the effective oligomer length in MEH-PPV is $n \sim 5$. We note, however, that the authors of Ref. 28 recently reported TDDFT results for a series of polyene oligomers which suggest that B3LYP/TDDFT underestimates excitation energies to the lowest $1B_u$ state by 0.5 eV. Theoretical excitation energies to the lowest triplet state are also somewhat too low. More work is needed to benchmark the accuracy of the TDDFT approximations for analogous systems for specific finite chains.

The first excited singlet in the Pt species is the doubly degenerate E_u state corresponding to the well-known *Q* band of metalloporphyrins. It is computed to be at 2.49 eV, in excellent agreement with experiment.[29] The analogous triplet state is at 1.98 eV, also in good agreement with experiment[29] (compare these with the absorption and emission spectra in Fig. 2). B3LYP/TDDFT has been shown to be very effective in describing the excited states of free-base porphyrin and the simplest metallo-porphyrin, magnesium porphyrin.[30] Nguyen and Pachter[31] recently showed that TDDFT provides a good account of the spectrum of Zn porphyrin and substituted analogues. These studies, along with the present results for Pt(porphyrin), are quite encouraging given the complications associated with correlation effects in transition metal complexes.

IV. EXCITATION MECHANISMS

The possible phosphor excitation mechanisms can best be understood by considering the charged and neutral excitations of the polymer host and the phosphor dopant. Schematic electron energy (a) and neutral excitation (b) diagrams for BCHA and PtOEP, derived from model molecular calculations, are shown in Fig. 5. For the phosphor to capture an electron, the electron affinity of the host, $\mathcal{E}_h$, must be smaller than the electron affinity of the dopant, $\mathcal{E}_d$, and for the phosphor to capture a hole the ionization potential of the host, $\mathcal{I}_h$, must be larger than the ionization potential of the dopant, $\mathcal{I}_d$. Dexter and Förster transfer processes both involve the transfer of a neutral excitation from the host BCHA to the dopant

PtOEP. In order for a Dexter transfer to occur, the energy of the first excited triplet in the host, $T_{1,h}$, must be greater than the energy of the first excited triplet in the dopant, $T_{1,d}$. Similarly, for a Förster process to occur, the energy of first excited singlet in the host, $S_{1,h}$, must be greater than the energy of the first excited singlet in the dopant, $S_{1,d}$. The molecular calculations are useful to determine if these processes can occur. For the $n=5$ oligomer, $\mathcal{E}_h-\mathcal{E}_d=-0.02$ eV, $\mathcal{I}_h-\mathcal{I}_d=-1.56$ eV, $T_{1,h}-T_{1,d}=-0.44$ eV, and $S_{1,h}-S_{1,d}=-0.07$ eV. Based on these excitation energy differences, it is unlikely that Dexter excitation transfer or hole capture by PtOEP can occur. However, given the accuracy of the molecular calculations, the energy difference between the singlet excitations is too small to rule out Förster transfer and, similarly, the energy difference between the electron affinities is too small to rule out electron capture by PtOEP. Although electron capture by PtOEP may occur, the large energy barrier to hole capture suggests that sequential charge capture is not a likely process. Therefore, based on the molecular calculations, the most likely phosphor excitation mechanism is Förster transfer. Theoretical calculations can be used to design systems in which Dexter and charge-transfer excitations are dominant.

To determine the excitation transfer mechanism experimentally, a series of measurements of the material and device structures were performed. The built-in potentials of device structures were measured to determine if the metal/organic Schottky energy barriers were altered by the phosphor doping. The metal/organic Schottky barrier could be modified by charge transfer to the phosphor dopant or by an interfacial chemical reaction with the phosphor.[11] The electron and hole transport properties were assessed by measuring the current-voltage characteristics of hole-dominant and electron-only devices. If the phosphor molecule has either an electron or hole energy level in the energy gap of the polymer, then the respective charge-carrier mobility would be substantially reduced.[11] If charge-carrier capture by the phosphor occurs, then the Schottky energy barriers and/or the carrier mobility would be changed. The T_1-T_N absorption peak of the polymer was measured in the diodes. If there was a significant transfer of triplet excitons from the polymer to the phosphor (Dexter transfer) then the amplitude of the T_1-T_N absorption peak, which is a measure of the triplet population in the polymer, should decrease. Finally, phosphor-doped devices were made using a closely related polymer with similar electronic structure, but with a redshifted emission that does not overlap the absorption spectrum of the phosphor. Since the absorption and emission spectrum[10] do not overlap, the Förster energy-transfer process is not allowed in this case. These measurements probe the excitation transfer processes individually, allowing the dominant mechanism to be identified.

At zero bias in a fully depleted metal/organic/metal structure there is a built-in potential in the device equal to the difference between the electron Schottky energy barriers of the two metal contacts.[11] The electroabsorption signal as a function of bias voltage was measured to determine the built-in potential in undoped and PtOEP-doped BCHA devices. The electroabsorption signal at the fundamental frequency of the applied ac bias is proportional to the electric field in the structure, which can be nulled by application of an external dc bias. The built-in potential in the structure is the bias at which the electroabsorption signal is a minimum. Figure 6 shows the electroabsorption signal as a function of dc bias voltage for undoped and PtOEP-doped Pt/Ca devices. The built-in potential is about 2.2 V in both structures. This demonstrates that PtOEP doping does not change either the Pt or Ca Schottky energy barrier. Because the Schottky barrier does not change with PtOEP doping, this implies that PtOEP does not introduce energy levels that are deep in the energy gap of BCHA, and that reactions between the contact metals and the PtOEP do not change the Schottky barrier between the contact metals and the polymer. These Schottky energy barriers must be determined independently from current-voltage (I-V) measurements in order to use I-V characteristics (see below) to assess the changes in carrier mobility due to the dopant. If the Schottky energy barriers are not independently known, then changes in the I-V characteristics could be caused either by carrier trapping on the dopant or by changes in the Schottky barrier.

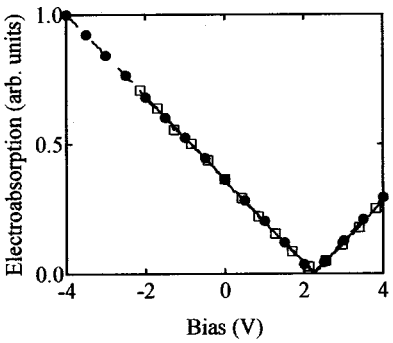

FIG. 6. Electroabsorption signal at the fundamental frequency of the applied ac bias as a function of bias for BCHA Pt/Ca (dashed, solid circle) and BCHA:PtOEP (20 wt %) (solid, open square) Pt/Ca diodes.

Figure 7 shows the current-voltage characteristics of a series of electron only and hole dominant devices with both undoped and PtOEP doped BCHA layers. There are three

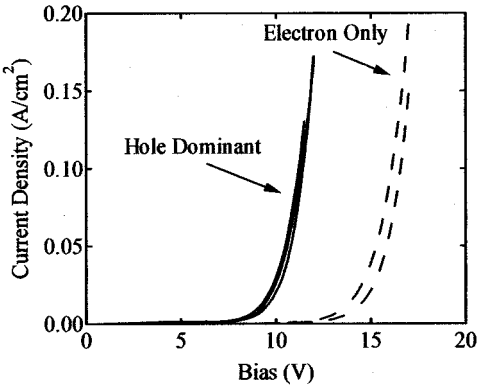

FIG. 7. Current-voltage characteristics of hole dominant (Pt/Ca, 0, 7, and 20 wt % PtOEP) and electron only (Al/Ca, 0 and 20 wt % PtOEP) BCHA:PtOEP diodes.

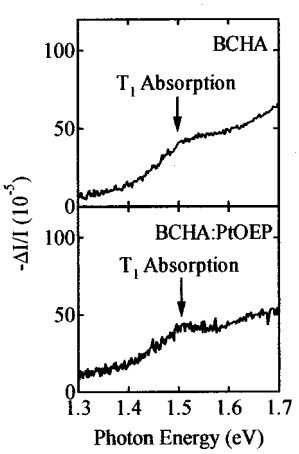

FIG. 8. Differential intensity spectra showing T_1-T_N absorption features in Pt/Ca diodes fabricated from BCHA (upper panel) and BCHA:PtOEP (20 wt %) (lower panel). The current density in each case was 1.0 A/cm^2.

Pt/Ca hole dominant current-voltage characteristics shown: 0 wt % PtOEP, 7 wt % PtOEP, and 20 wt % PtOEP. There are two Al/Ca electron only I-V characteristics shown: 0 wt % PtOEP and 20 wt % PtOEP. The I-V characteristics of the devices are not significantly altered by the presence of the PtOEP. This indicates that the PtOEP molecule does not act as an electron or hole trap that would modify the carrier mobility and thus the current-voltage characteristic of the device. It is essential to measure the electron and hole currents, and thus their transport properties, independently to determine that PtOEP does not act as a trap for either carrier type. Nominally bipolar I-V characteristics are often dominated by a single carrier type (e.g., holes), and therefore the bipolar I-V characteristic is not sensitive to changes in the minority carrier mobility (e.g., electrons) that would be introduced by carrier capture by the dopant.

Figure 8 shows the modulation of the diode optical properties, $-\Delta I/I$, under forward bias at a current density of 1 A/cm^2 for a PtOEP-doped and undoped Pt/Ca BCHA diodes. The modulated optical properties were measured using pulsed electrical excitation and phase-sensitive detection at room temperature. The incident light passed through a semitransparent Pt contact and a polymer layer, reflected off the thick Ca contact, and passed through the polymer layer and the transparent contact a second time. The modulated optical signal intensity $-\Delta I/I$ is proportional to $\Delta\alpha d$, where I is the incident intensity, $\Delta\alpha$ is the change in polymer absorption coefficient, and d is the film thickness.[32] The feature at about 1.5 eV in the modulated optical spectrum is the T_1-T_N absorption peak. The amplitude of the absorption peak is essentially the same in both the doped and undoped devices implying that the BCHA triplet population is not substantially affected by the presence of the PtOEP. Because the polymer triplet population is not affected by the dopant, this implies that Dexter transfer processes from the polymer triplet state to the phosphor are not significant. The calculated oscillator strength for the excited-state triplet absorption at 1.5 eV in the $n=5$ oligomer is 3.08. This oscillator strength corresponds to a peak absorption coefficient of 4 $\times 10^8$ cm^2/mole, determined assuming a rectangular triplet absorption peak 0.1 eV wide. Because the polymer chains lie predominantly in the plane of the film and the triplet transition dipole is oriented along the chain, the effective triplet absorption coefficient in the films is about 2 $\times 10^8$ cm^2 mole. The maximum measured $-\Delta I/I$ at the peak of the triplet absorption is about 5×10^{-5} in a 150-nm thick film. Based on the theoretical oscillator strength this corresponds to a triplet density of about 4×10^{14} cm^{-3}.

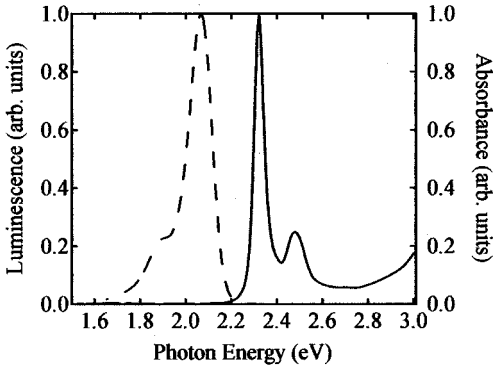

FIG. 9. Luminescence spectrum of MEH (dashed, left vertical axis) and absorbance spectrum of PtOEP (solid, right vertical axis).

These measurements show that sequential charge capture and Dexter transfer do not excite the PtOEP molecule. Combined with the measured spectral overlap between the BCHA emission and PtOEP absorption, this implies that Förster transfer produces the PtOEP excitation. To verify that Förster transfer is the only active process in this system, we examined poly[2-methoxy, 5-(2′-ethyl-hexyloxy)-1, 4-phenylene vinylene] (MEH) based diodes. MEH has an energy structure similar to BCHA, except that the emission spectrum of MEH is slightly red shifted with respect to BCHA. As shown in Fig. 9, the emission spectrum of MEH does not overlap the absorption spectrum of PtOEP and so Förster transfer processes are forbidden. Several MEH:PtOEP/Pt/Ca diodes, with PtOEP concentrations up to 40 wt %, were measured. For all PtOEP concentrations, no emission from the PtOEP dopant was observed, consistent with the conclusion that Förster transfer is the dominant active process in these systems. Based on our absorption and emission measurements, the calculated Förster transfer radius between BCHA and PtOEP is about 5 nm.[33] Therefore, a concentration of about 1 wt % PtOEP in BCHA should have equal emission intensity from BCHA and PtOEP. Experimentally, a concentration of about 7% was required to produce equal emission intensities. When emission from both PtOEP and BCHA is observed, the higher energy luminescence emission of BCHA is preferentially decreased. The emission spectrum of pure BCHA films is much broader than other polymers in the PPV family. This suggests that the emission from pure BCHA films is from an inhomogeneous energy distribution of emitting sites. The inhomogeneous energy distribution of emitting sites in the BCHA may account for the comparatively high concentration of PtOEP required for efficient Förster excitation transfer in this system.

V. SUMMARY

We presented experimental measurements and theoretical calculations of the electrical and optical properties of PtOEP-doped BCHA light-emitting diodes to determine the excitation transfer processes that lead to radiative recombination from PtOEP. Three possible excitation processes were considered: (1) sequential electron and hole capture, (2) Dexter energy transfer, and (3) Förster energy transfer. Built-in potential and current-voltage measurements indicate that the electron and hole energy levels of PtOEP are outside the energy gap of BCHA, and therefore that sequential electron and hole capture does not occur. Measurements of BCHA triplet optical absorption show that the triplet population in BCHA is not affected by the presence of PtOEP, indicating that Dexter transfer processes are weak. In the analogous polymer MEH, excitation transfer does not occur because there is no overlap between the emission spectrum of MEH and the absorption spectrum of PtOEP. These results demonstrate that the dominant active excitation transfer path from BCHA to PtOEP is Förster energy transfer. These conclusions are consistent with the charged and neutral electronic excitation energies of the polymer and phosphor determined by hybrid and time-dependent, density-functional-theory calculations.

ACKNOWLEDGMENTS

The work at Los Alamos was funded by the U.S. DOE Office of Building Technology and the Los Alamos National Laboratory LDRD program. I. H. C. thanks D. R. Brown for technical support and S. T. gratefully acknowledges the support of a LANL Director's Postdoctoral Fellowship. Portions of the numerical studies were performed at the Center for Nonlinear Studies at Los Alamos National Laboratory.

[1] C. Adachi, M. A. Baldo, S. R. Forrest, and M. E. Thompson, Appl. Phys. Lett. **77**, 904 (2000).

[2] M. A. Baldo, M. E. Thompson, and S. R. Forrest, Nature (London) **403**, 750 (2000).

[3] R. C. Kwong, S. Lamansky, and M. E. Thompson, Adv. Mater. **12**, 1134 (2000).

[4] C. Adachi, M. A. Baldo, S. R. Forrest, S. Lamansky, M. E. Thompson, and R. C. Kwong, Appl. Phys. Lett. **78**, 1622 (2001).

[5] N. C. Greenham and R. H. Friend, in *Solid State Physics*, edited by H. Ehrenreich and F. Spaepen (Academic, New York, 1955), Vol. 49, pp. 1–149.

[6] C. L. Gettinger, A. J. Heeger, J. M. Drake, and D. J. Pine, Mol. Cryst. Liq. Cryst. Sci. Technol., Sect. A **256**, 507 (1994).

[7] B. H. Cumpston and K. F. Jensen, Synth. Met. **73**, 195 (1995).

[8] D. F. O'Brien, C. Giebler, R. B. Fletcher, A. J. Cadby, L. C. Palilis, D. G. Lidzey, P. A. Lane, D. D. C. Bradley, and W. Blau, Synth. Met. **116**, 379 (2001).

[9] D. F. O'Brien, M. A. Baldo, M. E. Thompson, and S. R. Forrest, Appl. Phys. Lett. **74**, 442 (1999).

[10] I. H. Campbell, T. W. Hagler, D. L. Smith, and J. P. Ferraris, Phys. Rev. Lett. **76**, 1900 (1996).

[11] I. H. Campbell and D. L. Smith, in *Solid State Physics*, edited by H. Ehrenreich and F. Spaepen (Academic Press, New York, 2001), Vol. 55, pp. 1–117.

[12] M. Hopmeier, W. Guss, M. Deussen, E. O. Govel, and R. F. Mahrt, Phys. Rev. Lett. **82**, 4118 (1999).

[13] P. Andrew and W. L. Barnes, Science **290**, 785 (2000).

[14] S-K. Lee and I. Okura, Anal. Chim. Acta **342**, 181 (1997).

[15] A. D. Becke, J. Chem. Phys. **98**, 5648 (1993); A. D. Becke, in *Modern Electronic Theory*, edited by D. A. Yarkony (World Scientific, Singapore, 1995), Pt. II.

[16] M. E. Casida, in *Recent Advances in Density Functional Methods*, edited by D. P. Chong (World Scientific, Singapore, 1995), Vol. 1.

[17] M. E. Casida, in *Recent Developments and Applications of Modern Density Functional Theory, Theoretical and Computational Chemistry*, edited by J. M. Seminario (Elsevier, Amsterdam, 1996).

[18] M. Petersilka, U. J. Grossmann, and E. K. U. Gross, Phys. Rev. Lett. **76**, 1212 (1996); M. Petersilka and E. K. U. Gross, Int. J. Quantum Chem. Quantum Chem. Symp. **30**, 181 (1996).

[19] R. Bauernschmitt and R. Ahlrichs, Chem. Phys. Lett. **256**, 454 (1996); R. Bauernschmitt, R. Ahlrichs, F. H. Hennrich, and M. M. Kappes, J. Am. Chem. Soc. **120**, 5052 (1998).

[20] R. E. Stratmann, G. E. Scuseria, and M. J. Frisch, J. Chem. Phys. **109**, 8218 (1998).

[21] Gaussian 98, Revision A.9, M. J. Frisch, G. W. Trucks, H. B. Schlegel, G. E. Scuseria, M. A. Robb, J. R. Cheeseman, V. G. Zakrzewski, J. A. Montgomery, Jr., R. E. Stratmann, J. C. Burant, S. Dapprich, J. M. Millam, A. D. Daniels, K. N. Kudin, M. C. Strain, O. Farkas, J. Tomasi, V. Barone, M. Cossi, R. Cammi, B. Mennucci, C. Pomelli, C. Adamo, S. Clifford, J. Ochterski, G. A. Petersson, P. Y. Ayala, Q. Cui, K. Morokuma, D. K. Malick, A. D. Rabuck, K. Raghavachari, J. B. Foresman, J. Cioslowski, J. V. Ortiz, B. B. Stefanov, G. Liu, A. Liashenko, P. Piskorz, I. Komaromi, R. Gomperts, R. L. Martin, D. J. Fox, T. Keith, M. A. Al-Laham, C. Y. Peng, A. Nanayakkara, C. Gonzalez, M. Challacombe, P. M. W. Gill, B. Johnson, W. Chen, M. W. Wong, J. L. Andres, C. Gonzalez, M. Head-Gordon, E. S. Replogle, and J. A. Pople, Gaussian, Inc., Pittsburgh, PA, 1998.

[22] R. L. Martin, J. D. Kress, I. H. Campbell, and D. L. Smith, Phys. Rev. B **61**, 15 804 (2001).

[23] D. Mukhopadhyay, G. W. Hayden, and Z. G. Zoos, Phys. Rev. B **51**, 9476 (1995).

[24] J. L. Bredas, J. Cornil, D. Beljonne, D. A. Dos Santos, and Z. Shuai, Acc. Chem. Res. **32**, 267 (1999).

[25] S. Tretiak, V. Chernyak, and S. Mukamel, Int. J. Quantum Chem. **70**, 711 (1998).

[26] A. P. Monkman, H. D. Burrows, M. da G. Miguel, I. Hamblett, and S. Navaratnam, Chem. Phys. Lett. **307**, 303 (1999).

[27] L. P. Candeias, J. Wildeman, G. Hadziioannou, and J. M. Warman, J. Phys. Chem. B **104**, 8366 (2000).

[28] C. Hsu, S. Hirata, and M. Head-Gordon, J. Phys. Chem. A **105**, 451 (2001).
[29] D. H. Kim, D. Holten, M. Gouterman, and J. W. Buchler, J. Am. Chem. Soc. **106**, 4015 (1984).
[30] D. Sundholm, Chem. Phys. Lett. **317**, 392 (2000); Phys. Chem. Chem. Phys. **2**, 2275 (2000).
[31] K. A. Nguyen and R. Pachter, J. Chem. Phys. **114**, 10 757 (2001).
[32] I. H. Campbell, D. L. Smith, C. J. Neef, and J. P. Ferraris, Phys. Rev. B **64**, 035203 (2001).
[33] T. Förster, Discuss. Faraday Soc. **27**, 7 (1959).